The Journal of Navigation (2022), **75**:3 540–553
doi:10.1017/S037346332100059X

CAMBRIDGE UNIVERSITY PRESS

RESEARCH ARTICLE

A novel partial ambiguity method for multi-GNSS real-time kinematic positioning

Haiyang Li, Guigen Nie,* Jing Wang, Shuguang Wu, and Yuefan He

GNSS Research Center, Wuhan University, Wuhan, China.
*Corresponding author. E-mail: ggnie@whu.edu.cn

Received: 27 January 2021; **Accepted:** 21 June 2021; **First published online:** 15 July 2021

Keywords: RTK, partial ambiguity resolution, initial ambiguity resolution, irrespective of integer ambiguity resolution

Abstract

Recent progress in using real-time kinematic (RTK) positioning has motivated the exploration of its application due to its high accuracy and efficiency. However, poorly-observed satellite data will cause unfixed ambiguities and markedly biased solutions. A novel partial ambiguity resolution method, named the irrespective of integer ambiguity resolution (IIAR) model, is proposed and applied to improve the reliability of ambiguity resolution. The proposed method contains initial ambiguity resolution and irrespective of integer ambiguity processes. The initial ambiguity resolution process applies an iterative partial ambiguity resolution method to obtain an approximate solution. The irrespective of integer ambiguity process transforms the approximate solution to a high-precision solution. Experiments show that the approximate solution is unreliable when the initial ambiguity resolution process has small redundancy, and the proposed method can obtain better results for those cases. The IIAR method showed about a 40% improvement of multi-GNSS ambiguity success rate and about a 25% improvement of standard deviation. Therefore, these results show that the proposed IIAR method can improve the results of multi-GNSS RTK positioning significantly.

1. Introduction

In recent years, real-time kinematic (RTK) positioning has been successfully used in many fields for its characteristics of rapid positioning, not accumulating error, and high efficiency. However, the integer ambiguity resolution turns out to have a big impact on RTK positioning. Solutions with fixed ambiguities can make it possible to achieve positioning precision at the millimetre level (Zhodzishsky et al., 1998; Edwards et al., 1999; Teunissen, 1999; Odolinski et al., 2015). Since the 1990s, many studies have been conducted to resolve the integer ambiguity (Position Location and NaTeunissen, 1994; Ge et al., 2005; Feng, 2008; Xu et al., 2012). Multiple systems with multiple frequencies prove to be an effective method to improve the ambiguity success rate (Wang and Feng, 2013; Deng et al., 2014; He et al., 2014; Odolinski et al., 2015; Paziewski and Wielgosz, 2015; Torre and Caporali, 2015). But poorly-observed satellite data will result in unfixed ambiguities in multi-GNSS RTK positioning. The partial ambiguity resolution method is developed to solve this problem (Teunissen et al., 1999).

Several partial ambiguity resolution methods have been proposed to solve this problem (Dai et al., 2007; Takasu and Yasuda, 2010; Parkins, 2011; Wang and Feng, 2013; Li et al., 2015). The first group of methods select an ambiguity subset by signal-to-noise (SNR) (Parkins, 2011) and elevation angle (Takasu and Yasuda, 2010). Multi-GNSS RTK positioning contains poorly-observed satellite data with larger noise and residuals. The ambiguity resolution success rate can be improved by removing these poorly-observed data. The second group of methods select a narrow-lane ambiguity subset with smaller variances (Li et al., 2015). After wide-lane ambiguity is fixed, a partial narrow-lane ambiguity resolution

© The Author(s), 2021. Published by Cambridge University Press on behalf of The Royal Institute of Navigation

https://doi.org/10.1017/S037346332100059X Published online by Cambridge University Press

method is developed to improve the success rate. The third group of methods select the optimal subset of the ambiguity projections (Wang and Feng, 2013). After ambiguity decorrelation, some rules are used to select the optimal subset in the ambiguity projections to improve the success rate. Those partial ambiguity resolution methods select suitable ambiguity subsets by different rules. Consequently, they have their own merits.

Against this background, this paper presents a new partial ambiguity resolution strategy – the IIAR method, containing the initial ambiguity resolution and the IIAR processes. The initial ambiguity resolution process is to obtain an approximate solution, but the pseudo-range single point positioning (SPP) float solution cannot meet the requirements. To resolve this problem, the initial ambiguity resolution process applies an iterative partial ambiguity resolution to obtain the approximate solution and set it as the virtual fixed solution. This virtual fixed solution is then set as the solution of the virtual station. Previous studies applied the partial ambiguity resolution method for poorly-observed data, but its solution is unreliable when the selected satellites have poor geometry. To solve this problem, the irrespective of ambiguity resolution process resolves all the adjustment equations. It is hypothesised that the virtual station and the estimated rover station have the same integer ambiguities in RTK positioning. With the virtual fixed solution, all of the adjustment equations are transformed into a new form. The proposed IIAR method omits the integer ambiguity resolution for poorly-observed satellites and improves the situation in which the selected satellites have poor geometry. This study is structured as follows. First, the IIAR method is introduced in detail, then the method is validated with real data and the results are analysed in order to reach the conclusion.

2. Method

In this section, the principle of the IIAR method is described in detail.

2.1. Initial ambiguity resolution process

There are more available satellites for multi-GNSS positioning. It is difficult to fix ambiguities for all the satellites, however, because of multipath and atmospheric residuals. The partial ambiguity resolution method is developed to solve this problem. But its solution is unreliable when few satellites are available for partial ambiguity resolution. This section presents the application of an iterative partial ambiguity resolution method to obtain an approximate solution like Site B in Figure 1.

GNSS observation equation is expressed as follows:

$$Y = AX + Bb + \varepsilon \tag{1}$$

where $Y \in R^m$ denotes the vector of the pseudo-range and carrier phase observation; $A \in R^{m*n}$ denotes the matrix of designed coefficients; $X \in R^n$ denotes the vector of the estimated coordinates; $B \in R^{m*p}$ denotes the matrix of carrier phase length; $b \in Z^p$ denotes the vector of the estimated integer ambiguity; $\varepsilon \in R^m$ denotes the noise vector, which is assumed to follow a zero-mean Gaussian distribution. The float solution of X and b and their variance matrices are expressed as follows:

$$\begin{bmatrix} X_f \\ b_f \end{bmatrix} \quad \begin{bmatrix} Q_{11} & Q_{12} \\ Q_{21} & Q_{22} \end{bmatrix} \tag{2}$$

where $b_f \in R^p$ denotes the float solution vector of b; $X_f \in R^n$ denotes the float solution vector of X; $Q_{11} \in R^{n*n}$ denotes the variance submatrix of coordinates; $Q_{22} \in R^{q*q}$ denotes the variance submatrix of ambiguity; $Q_{12} \in R^{n*q}$ and $Q_{21} \in R^{q*n}$ denote the covariance submatrices.

Integer ambiguity resolution is essential for RTK positioning. It is difficult to fix ambiguities for all the satellites in a complex environment, so partial ambiguity resolution is implemented (Teunissen, 1999, 2001; Teunissen et al., 1999). The key for partial ambiguity resolution is to select a feasible

https://doi.org/10.1017/S037346332100059X Published online by Cambridge University Press

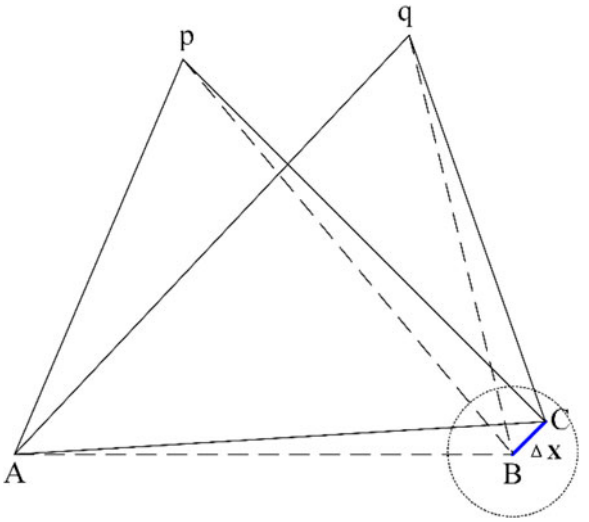


Figure 1. *Schematic diagram of the IIAR method.*

ambiguity subset. An ambiguity subset is fixed, with a bootstrapped success rate greater than or equal to a minimum required value P_0, to select the feasible subset such that:

$$F(b) = \prod_{i=k}^{p} \left(2\Phi\left(\frac{1}{2\sigma_{b_{i|I}}} - 1\right)\right) \geq P_0 \tag{3}$$

where $\Phi(x)$ denotes the cumulative normal distribution; $\sigma_{b_{i|I}}$ denotes the conditional variance element; $b_{i|I} \in R^{p-i+1}$ denotes the feasible ambiguity subset. Equation (3) denotes that only the last $p - k + 1$ ambiguities are in the feasible subset. The ambiguity resolution is then applied for the selected subset.

Many studies have been conducted to resolve the integer ambiguity, such as integer least-squares (Teunissen, 1999), integer bootstrapping (Teunissen, 1998) and integer rounding (Jonge and Tiberius, 1998). The formula of integer least-squares ambiguity resolution is expressed as follows:

$$f(\nabla\Delta b) = \min\left(\nabla\Delta b - \nabla\Delta b_f\right)^T Q_{22}\left(\nabla\Delta b - \nabla\Delta b_f\right) \tag{4}$$

where $\nabla\Delta$ denotes the double-difference symbol. This estimator is known to be optimal, which means the probability of the correct integer estimation is maximised (Teunissen, 1999). In this study, the least-squares ambiguity decorrelation adjustment (LAMBDA) method is used to resolve ambiguities for the selected satellites (Teunissen, 1995). The initial ambiguity resolution process is an iterative partial ambiguity resolution method. The iterative model guarantees the correctness of the virtual station. Equation (4) is the criterion of the partial ambiguity resolution. The iterative model will end if the adjacent iterations have the same ambiguity subsets.

The initial ambiguity resolution is to obtain an approximate solution, which is set as the virtual fixed solution of the virtual station. Previous studies apply the iterative partial ambiguity resolution method to obtain the solution, but the solution is unreliable when the selected satellites have small redundancy. This study applied an iterative partial ambiguity resolution to obtain the virtual fixed solution, and the iteration will end when the adjacent iterations have the same ambiguity subsets. The virtual fixed solution is unreliable for high-precision positioning, and the IIAR process is essential.

https://doi.org/10.1017/S037346332100059X Published online by Cambridge University Press

2.2. IIAR process

The initial ambiguity resolution process applies an iterative partial ambiguity resolution method to obtain the virtual fixed solution, which omits the ambiguity resolution for poorly-observed satellites. It is hypothesised that the virtual station and the estimated rover station have the same integer ambiguities in RTK positioning. There is no need to resolve integer ambiguities for other satellites with the virtual fixed solution. The IIAR process transforms all of the adjustment equations to a new form. More formula derivations are given in the following section.

Figure 1 illustrates a double-difference for site B and site C in. According to Equation (1), the double-difference ambiguity formula for each observation equation is expressed as follows:

$$\nabla\Delta b_i = \text{Round}\left(\nabla\Delta\varphi_i - \frac{\nabla\Delta\rho_i}{\lambda_i}\right) \tag{5}$$

where i denotes the frequency i; $\nabla\Delta b_i$ denotes the double-difference ambiguity element; Round$(\cdot)$ denotes the rounding function; $\nabla\Delta\varphi_i$ denotes the double-difference carrier phase observation element; $\nabla\Delta\rho_i$ denotes the double-difference pseudo-range observation element; λ_i denotes the carrier phase length element of frequency i. Zhang et al. (2003) applied Equation (5) for short baseline monitoring. They obtained the estimated solution based on the hypothesis that the current epoch had the same integer ambiguities as the initial epoch. In the presetn study, the equation is applied to substitute the integer ambiguities based on the initial ambiguity resolution process. The selected observations in the initial ambiguity resolution process and the remaining observations are used to make double differences for Equation (5). The integer bootstrapping estimator is a sequential least-squares adjustment. It starts with the more precise ambiguity, here assumed to be the last ambiguity, and rounds its value to the nearest integer. By contrast, the proposed model divides the ambiguities into two parts. The selected observations in the initial ambiguity resolution process obtain the virtual fixed solution. This solution is unreliable with a small redundancy. The remaining observations eliminate the ambiguities by Equation (5) to obtain a larger redundancy.

Equation (5) is aimed at the code division multiple access model. As for the frequency division multiple access model, the double-difference ambiguity of GLObal NAvigation Satellite System (GLONASS) is not an integer. To solve this problem, the formula of Equation (5) is expressed as follows:

$$\lambda_i\Delta b_i - \lambda_j\Delta b_j = \lambda_i(\Delta b_i - \Delta b_j) + \Delta b_j(\lambda_i - \lambda_j) = \lambda_i\nabla\Delta b_{ij} + \Delta\lambda_{ij}\Delta b_j \tag{6}$$

where j denotes the frequency j; Δb_i denotes the single-difference ambiguity element of frequency i; Δb_j denotes the single-difference ambiguity element of frequency j; λ_j denotes the carrier phase length element of frequency j; $\nabla\Delta b_{ij}$ denotes the double-difference element of frequency i and j; $\Delta\lambda_{ij}$ denotes the single-difference element of frequency i and j. To solve the problem of the satellite geometry, Equations (5) and (6) are aimed at all of the observation equations. Teunissen (2019) proposed a new GLONASS ambiguity resolution model. The authors will apply this model to the proposed method in future studies.

Equation (6) has a new residual $\Delta\lambda_{ij}\Delta b_j$, which is influenced by the single-difference carrier phase length $\Delta\lambda_{ij}$ and single-difference integer ambiguity Δb_j. The new residual $\Delta\lambda_{ij}\Delta b_j$ is less than 0·1 cycle, in the condition that $\Delta\lambda_{ij}$ is minimal or Δb_j is more than several cycles (Zhang et al., 2001), and $\Delta\lambda_{ij}\Delta b_j$ is absorbed into double-difference noise $\nabla\Delta\varepsilon$. According to Equations (1), (5) and (6), the formula for each double-difference observation equation is as follows:

$$A_i\Delta X = \lambda_i\nabla\Delta\varphi_i - \nabla\Delta\rho_i - \lambda_i Round\left(\nabla\Delta\varphi_i - \frac{\nabla\Delta\rho_i}{\lambda_i}\right) - \nabla\Delta\varepsilon_i \tag{7}$$

https://doi.org/10.1017/S037346332100059X Published online by Cambridge University Press

where $A_i \in R^{m*n}$ denotes the designed matrix for Equations (5) and (6); $\Delta X \in R^n$ denotes the difference vector between the virtual station and the estimated station. The coordinate formula is then as follows:

$$X_{cs} = X_{vfs} + \Delta X \tag{8}$$

where $X_{cs} \in R^n$ denotes the current solution vector. The IIAR process obtains the difference vector ΔX, and then the current solution vector X_c will be output if ΔX meets the requirement. The proposed method divides the observations into two parts. The selected observations in the initial ambiguity resolution process obtain a range solution, while the IIAR process obtains a high-precision solution with larger redundancy. It is hypothesised that the virtual fixed solution and the final solution have the same double-difference ambiguities. The selected observations are used to eliminate the integer ambiguity parameters of the remaining observations. The biases in the remaining observations will be decreased or eliminated by Equations (5) and (6).

Different from the previous studies, this method transforms the integer ambiguity into a new form. It is hypothesised that the virtual station and the estimated rover station have the same integer ambiguities in RTK positioning. With the virtual fixed solution, the integer ambiguity vector is substituted by the pseudo-range and carrier phase observation. The IIAR process resolves the adjustment equations for all the satellites, which solves the problem of poor satellite geometry.

2.3. Threshold of the difference vector ΔX

Equations (5) and (8) indicate that ΔX should be within a certain range. It is hypothesised that the virtual station and the estimated rover station have the same integer ambiguities in RTK positioning. That means their difference is less than half wavelength. The formula is expressed as follows:

$$|A_i \Delta X| \leq 0 \cdot 5\lambda \tag{9}$$

Supposing that maximum displacements for E (east), N (north) and U (up) are equal, Equation (8) is derived as follows (Liu, 2014):

$$|\Delta X| \leq \frac{\sqrt{3} \cdot 0 \cdot 5\lambda_i}{MAX(|A_i|^2)} = \frac{\sqrt{3} \cdot 0 \cdot 5\lambda_i}{\sqrt{2}} = 0 \cdot 6\lambda_i \tag{10}$$

where $|A_i|$ denotes the determinant value of A_i. According to Equations (8) and (10), the formula is expressed as follows:

$$|\Delta X| = |X - X_{pre}| < 0 \cdot 6\lambda_i \tag{11}$$

where X_{pre} denotes the solution in the previous iteration. The difference between X and X_{pre} should satisfy Equation (11). But the SPP float solution X_f cannot meet this requirement. To obtain a more accurate solution, an iterative partial ambiguity resolution method is applied for the initial ambiguity resolution process, and its solution substitutes X_v for X_f. The proposed IIAR method obtains an approximate solution in the initial ambiguity process, while the irrespective of integer ambiguity process resolves the adjustment equations to obtain the high-precision estimated coordinates. It is hypothesised that the virtual station and the estimated rover station have the same double-difference ambiguities in RTK positioning. So the virtual fixed solution should meet the requirements in this section. Otherwise, it indicates that the iterative partial ambiguity resolution obtains a low-precision solution. the experiment in section 3.2 shows that the proposed model cannot guarantee a high-precision solution when the virtual fixed solution cannot meet Equation (11). For clarity, the algorithm schematic diagram is presented in Figure 1.

The detailed steps of the proposed method are as follows, where site A is the base station; site C is the rover station; sites p and q are the satellite p and q:

https://doi.org/10.1017/S037346332100059X Published online by Cambridge University Press

Table 1. *Statistics of experiment hardware.*

Station		1	2	3	4	5
Receiver	Type	Trimble Net R9	Trimble Net R9	Trimble Net R9	Trimble Net R9	Trimble Net R9
	Version	5·03	5·03	5·03	4·81	5·03
Antenna		Trimble Zephyr Geodetic 2	Trimble Zephyr Geodetic 2	Trimble Zephyr Geodetic 2	Trimble Zephyr Geodetic 2	Trimble Zephyr Geodetic 2

1. Select feasible satellites for the initial ambiguity resolution process. The site B in Figure 1 is set as the virtual station and the initial ambiguity resolution process obtains its solution X_{init}.
2. Update the float solution X_f and the corrections of the virtual station by X_{init}.
3. Set the current solution X_{init} as the virtual fixed solution X_{vfs}, if the adjacent iterations have the same ambiguity subsets. Otherwise, back to step 1.
4. Substitute the combination of carrier phase and pseudo-range observations for the integer ambiguity as Equation (5).
5. Obtain the difference solution ΔX as Equation (7), and update the current solution X_{cs}. Now the current solution X_{cs} is resolved by all the observed satellites.
6. Set the current solution X_{cs} as the final solution X. Go to step 7, if it meets the requirement of Equation (11). Otherwise, back to step 1.
7. Output X as the fixed solution, if $|X - X_{init}| < 0.6\lambda$. Otherwise, output X_{pre} as the float solution.

3. Experiments

Ambiguity success rate (Equation (12)) is an essential proportion to assess the integer ambiguity resolution method. The formula is expressed as follows:

$$P_{fixed} = \frac{N_r}{N_{total}} \times 100\% \tag{12}$$

where P_{fixed} denotes the successful rate of correctly fixed ambiguity; N_r denotes the epoch numbers of correctly fixed ambiguity; N_{total} denotes all of the epoch numbers in the experiment. In this study, 3 cm, 3 cm and 5 cm are set for the correctly fixed ambiguity threshold of E, N and U directions. The processing strategy in this section is conducted by single epoch.

3.1. Ultra-short baseline experiment

To verify the proposed IIAR method, experiments were conducted on the roof of the China Electric Research Institute, with 15 s interval GPS + BDS + Galileo + GLONASS + QZSS (L1 + L2) data from 0:00 to 24:00 on 7 November 2019 (GPST). The five stations are situated on the roof of a 40 m building with good observation conditions. The cut-off elevation mask is 10°. Because of the different firmware versions, the receiver of site 4 did not contain Galileo data. The GNSS receivers were Trimble Net R9. There are two parts in this section. The first part demonstrates that the virtual fixed solution (VFS) was insufficient for high-precision positioning in a complex environment, while the second part demonstrates that the proposed IIAR method is feasible. The antenna and receiver hardware is as shown in Table 1.

3.1.1. VFS experiment

Previous studies applied the partial ambiguity resolution method to obtain a better result, but its solution may be unreliable in a complex environment. To prove this hypothesis, the China Electric Research Institute Baseline 1-2 GPS experiment was conducted. Figure 2 shows the time series of this experiment.

https://doi.org/10.1017/S037346332100059X Published online by Cambridge University Press

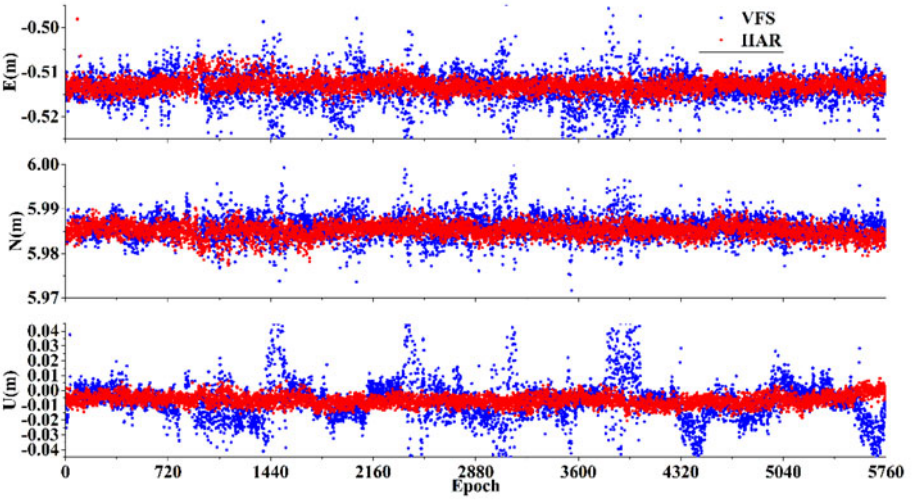


Figure 2. *Time-series scatter diagram of Baseline 1-2 GPS experiment.*

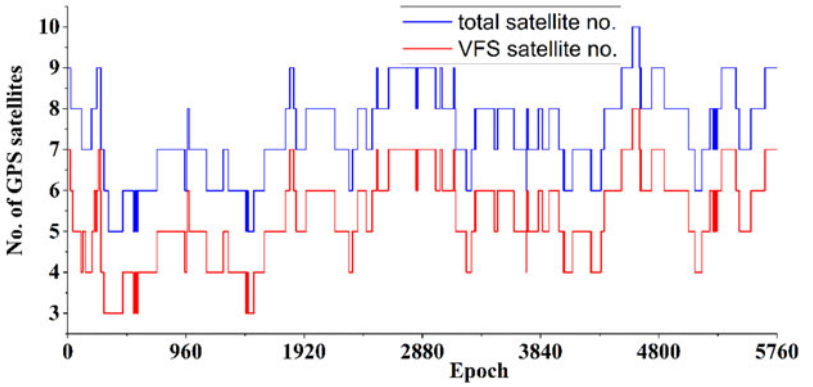


Figure 3. *Satellite time-series diagram of Baseline 1-2 GPS experiment.*

The experiment in this section was only conducted by GPS, which was more obvious to show that the VFS is not adequate for high-precision positioning. It could be seen that the time series of the VFS has many fluctuations, while the IIAR method had a smooth curve. For E directions, the time series of VFS had about 0·01 m fluctuations in about 1,400th, 2,000th, 2,500th, 2,900th, and 3,600th–4,000th epochs. For N directions, the time series of VFS had about 0·01 m fluctuations in about 500th, 1,400th, 2,500th, 2,900th, and 3,900th epochs, and about 0·005 m fluctuations in about 2,000th and 4,000th epoch. For U directions, the time series of VFS had about 0·04 m fluctuations in about 1,400th, 2,500th, 2,900th, 3,900th, 4,400th, and 5,700th epochs. It is known that RTK positioning can reach millimetre positioning accuracy for those ultra-short baseline experiments. So the VFS is not adequate for high-precision positioning. The VFS is obtained with small redundancy, while the IIAR is obtained with a larger redundancy. Figure 3 shows more details of this ultra-short baseline experiment.

Figure 2 shows the time series of the VFS and IIAR method in the China Electric Research Institute Baseline 1-2 GPS experiment. It was obvious that the VFS had many fluctuations, and the reason was shown in Figure 3. Figure 3 is the satellite time series diagram of the VFS experiment. The blue line is the total satellite number, while the red line is the selected satellite number. There were about seven satellites available during the experiment, but only about five satellites were feasible. Figure 2 shows that there were fluctuations in many epochs. Figure 3 shows that there were three feasible satellites in about the 500th and 1,400th epochs, and four feasible satellites in about the 2,500th, 2,900th, 3,900th,

https://doi.org/10.1017/S037346332100059X Published online by Cambridge University Press

Table 2. *Statistics of IIAR method, RTK method and total station.*

Baseline	System	Baseline length (m)		
		RTK	IIAR	Total station
1-2	BDS	6·0068	6·0072	6·0078
	GPS	6·0071	6·0072	
	Galileo	6·0105	6·0112	
	GLONASS	6·0063	6·0069	
	BDS + GPS + Galileo + GLONASS + QZSS	6·0070	6·0073	
3-2	BDS	6·0091	6·0093	6·0092
	GPS	6·0091	6·0100	
	Galileo	6·0073	6·0076	
	GLONASS	6·0092	6·0093	
	BDS + GPS + Galileo + GLONASS + QZSS	6·0098	6·0096	
4-2	BDS	5·9873	5·9873	5·9860
	GPS	5·9874	5·9873	
	GLONASS	5·9884	5·9884	
	BDS + GPS + GLONASS + QZSS	5·9875	5·9874	
5-2	BDS	6·0163	6·0165	6·0161
	GPS	6·0167	6·0160	
	Galileo	6·0338	6·0330	
	GLONASS	6·0163	6·0163	
	BDS + GPS + Galileo + GLONASS + QZSS	6·0159	6·0160	

4,400th and 5,700th epochs. The selected feasible satellite number corresponds to the fluctuations in Figure 2. The VFS experiment proved that the solution of the partial ambiguity resolution method is unreliable when the selected satellites have poor geometry.

3.1.2. Verification experiment

The Baseline 1-2 GPS experiment described in the above subsection proved that VFS was unreliable for high-precision positioning when the selected satellites have poor geometry. This subsection describes the Baseline 1-2 multi-GNSS experiment to verify the reliability of the proposed IIAR method. Table 2 shows the comparison of the IIAR method, RTK method and Leica TS60 total station results.

The experiment in this section is to make a comparison for the results of the RTK method, IIAR method and total station. The results of the total station are set as the criteria for the comparison of the RTK and IIAR methods. As for the Baseline 1-2 experiments, the BDS + GPS + Galileo + GLONASS + QZSS experiment had the best results with about 0·5 mm difference, and the Galileo experiment had the worst results with about 2·7 mm difference. Besides, BDS, GPS, and GLONASS experiments had similar results with about 0·8 mm difference. As for Baseline 3-2 experiments, BDS, GPS, GLONASS, and BDS + GPS + Galileo + GLONASS + QZSS experiments had the best results with about 0·3 mm difference, and the Galileo experiment had the worst results with about 1·6 mm difference. As for the Baseline 4-2 experiment, BDS, GPS and BDS + GPS + GLONASS + QZSS experiment had similar results with about 0·7 mm difference. The GLONASS experiment had the worst result with about a 2 mm difference. As for the Baseline 5-2 experiment, BDS, GPS, GLONASS and BDS + GPS + Galileo + GLONASS + QZSS experiments had similar results with about 0·5 mm difference, and the Galileo experiment had the worst results with about 2 mm difference. The IIAR method had a slight improvement in most cases, but there were some exceptions, such as the GPS experiment

https://doi.org/10.1017/S037346332100059X Published online by Cambridge University Press

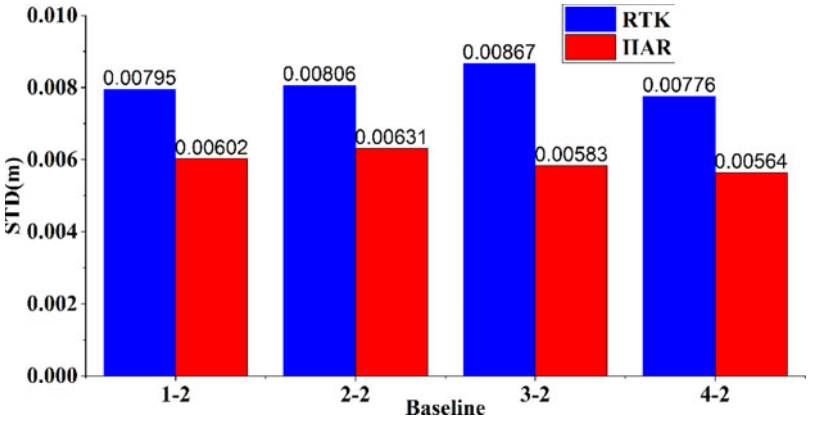


Figure 4. *STD statistic histogram for the four baseline multi-GNSS experiments.*

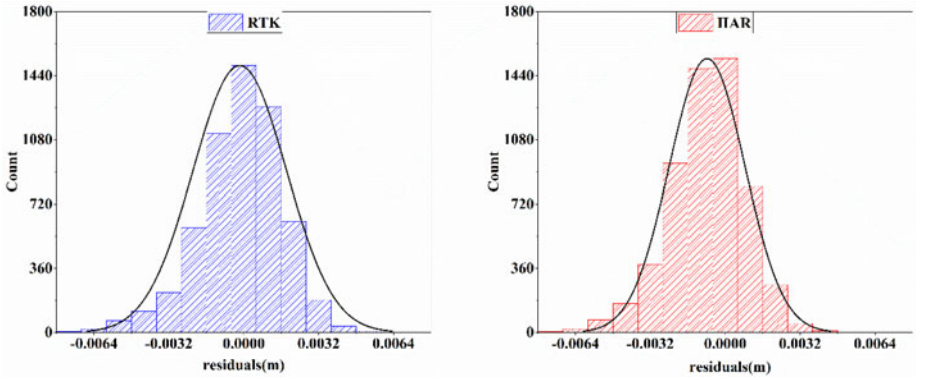


Figure 5. *Residual statistic histogram for Baseline 1-2 multi-GNSS experiment.*

of the Baseline 3-2 experiment, in which the RTK method had better results than the IIAR method. In summary, the IIAR method had a more precise solution than the RTK method in most cases.

Figure 4 shows the average standard deviation (STD) for the four baselines BDS + GPS + Galileo + GLONASS + QZSS experiment at the China Electric Research Institute. The IIAR method had noticeable improvement, compared with the RTK methods. In summary, the IIAR method had the most obvious improvement by about 25%, compared with the RTK method.

Figure 5 shows the comparison for the residual distribution of the Baseline 1-2 BDS + GPS + Galileo + GLONASS + QZSS experiment at the China Electric Research Institute. The left histogram in blue is the statistical results of the RTK method, while the right one in red is for the proposed IIAR method. The result of the IIAR method had more epochs in [−0·0032 m, 0·0032 m] than the RTK method. The IIAR method had a smaller variance, which corresponded to the statistical results in Figure 4. The verification experiment proved that the proposed IIAR method had slightly better results than the RTK method in the ultra-short baseline experiment.

3.2. Short baseline experiment

The experiment described in this subsection was to verify the practicality of the proposed IIAR method. The Wuhan Baishazhou Bridge S023 experiment was conducted with GPS + BDS + GLONASS (L1+L2) 10hz data, from 14:00 to 15:00 on 26 September 2016 (GPST). The length of the bridge is 3,598 m, while the width is 25·6 m. Site S023 is on the middle span of the bridge. The cut-off elevation mask is

https://doi.org/10.1017/S037346332100059X Published online by Cambridge University Press

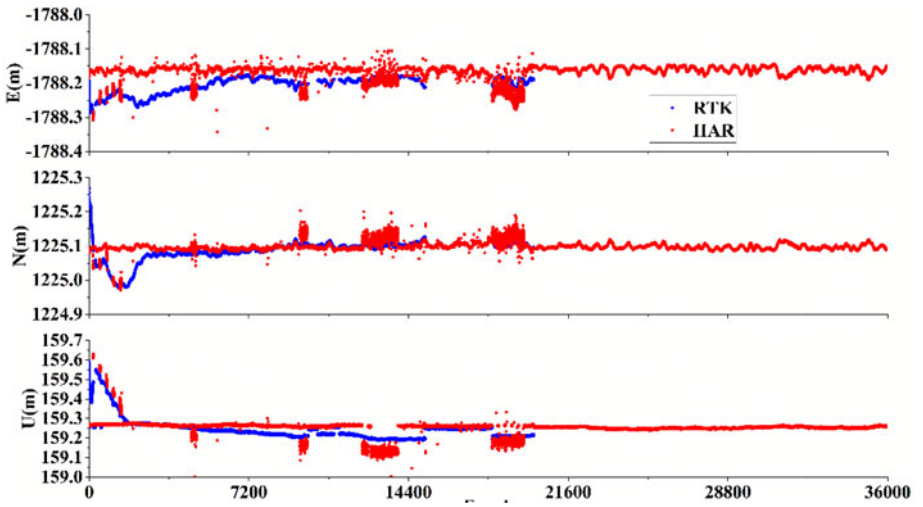


Figure 6. *Time-series scatter of Baishazhou Bridge S023 experiment.*

10°. The baseline length was 2,173·41 m. The GNSS receivers were ComNav-K508 and versions were 55·0. Figure 6 shows the time series of the Baishazhou S023 experiment.

The purpose of this experiment was to apply the proposed IIAR method to the bridge monitoring experiment. Figure 6 shows the comparison of the RTK method and the IIAR method. The IIAR method had obvious better results in the initial stage, while the RTK method had divergence. The RTK method could not obtain a fixed solution because of poorly-observed satellites therein. In contrast, the IIAR method had better convergence during the initial time with few fluctuations. But the IIAR method had worse results in about the 10,000th, 14,000th and 18,000th epochs. Both methods had similar results after about the 22,000th epoch. To obtain more obvious comparisons, Table 3 shows the statistics of the Baishazhou Bridge S023 experiment. These are: ambiguity success rate (ASR), time-to-first-fixed epoch (TTFF), and root mean squared error (RMSE). It was obvious that the IIAR method had better statistical results. For ASR, the GPS and BDS experiments had the same results. The GLONASS experiment was from 46·37% to 61·62%, and the multi-GNSS experiment was from 55·03% to 92·61%. For TTFF, the GPS and BDS experiments had the first fixed epoch in the first epoch. The GLONASS experiment had worse results than the GPS and BDS experiments. The RTK method had the first fixed epoch in the 9,400th epoch, while the IIAR method was in the 2,934th epoch. The results of the multi-GNSS experiment had better results than the GLONASS experiment. The RTK method had the first epoch in the 216th epoch, while the IIAR method was in the first epoch. For RMSE, the GLONASS experiment had the worst results in the four experiments, while the GPS experiment had the best results. It was obvious that the IIAR method had smaller RMSE results than the RTK method. In summary, the IIAR method had better results in the short baseline experiment.

Figure 7 is the time series statistic diagram of the Baishazhou Bridge S023 experiment, which shows the reason for Figure 6. Figure 6 shows that the RTK method had divergence results in the initial time, in which Figure 7 shows that there were about four poorly-observed satellites. The IIAR method had convergence results because the VFS was obtained by the selected feasible satellites. Figure 6 shows the IIAR method had worse results in about the 10,000th, 14,000th and 18,000th epochs, in which Figure 7 shows that the VFS was obtained by poor ratio value. Both methods had similar results after about the 22,000th epoch in Figure 6, in which Figure 7 shows that the VFS was obtained by better ratio value.

The short baseline experiment in this section shows that there are two keys to the proposed method. One is that the VFS must meet the requirement of Equation (13), and the other is that the residual had no impact on Equations (7) and (8).

https://doi.org/10.1017/S037346332100059X Published online by Cambridge University Press

Table 3. *Statistics of the Baishazhou Bridge S023 experiment.*

Method	Satellite system	ASR (%)	TTFF	RMSE (m)		
				E	N	U
RTK	GPS	99·62	1	0·00007	0·00005	0·00011
	BDS	99·61	1	0·00014	0·00022	0·00037
	GLONASS	46·37	9,400	0·12929	0·00846	0·15234
	GPS + BDS + GLONASS	55·03	216	0·00914	0·00884	0·00201
IIAR	GPS	99·62	1	0·00007	0·00004	0·00007
	BDS	99·61	1	0·00013	0·00016	0·00012
	GLONASS	61·62	2,934	0·08407	0·00594	0·09338
	GPS + BDS + GLONASS	92·61	1	0·00627	0·00060	0·00188

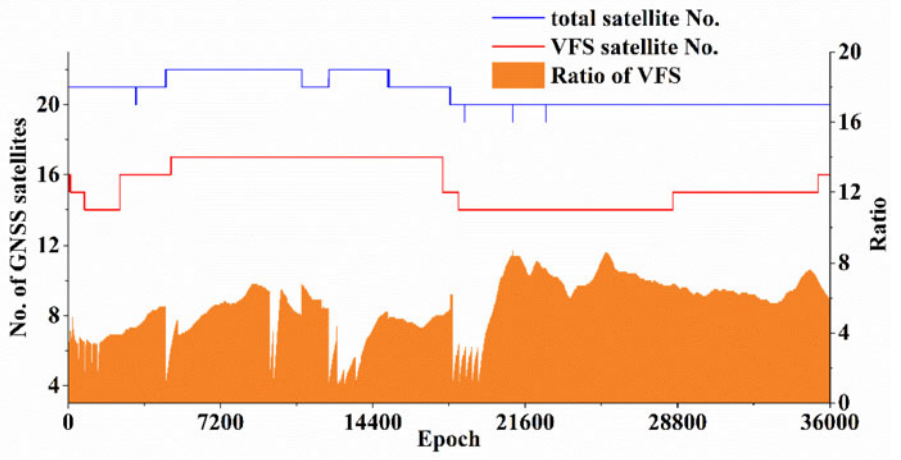


Figure 7. *Time-series statistic diagram of Baishazhou Bridge S023 experiment.*

3.3. Medium baseline experiments

The above two experiments focus on the short baseline experiments, and the experiment in this section was to verify whether the proposed IIAR method was feasible for the medium baseline experiment. Site 1 at the China Electric Research Institute was set as the rover station, while the Beijing Fangshan (bjfs) IGS site was set as the base station. The baseline length was 61,443·96 m. The site 1 receiver is introduced in Table 1. The IGS station receiver type is Trimble Net R9, and its version is 4·85. Figure 8 shows the time series of the Baseline 1-bjfs experiment.

Figure 8 shows the IIAR results for the Baseline 1-bjfs experiment. Compared with Figure 2, the IIAR results had divergence for most of the epochs. The above short baseline experiments show that the VFS and residual are the keys for the proposed method. Figure 9 shows the reason for Figure 8.

Figure 9 is the VFS time series scatter of the Baseline 1-bjfs experiment. The VFS had divergence for most of the epochs, which can meet the requirement of Equation (13). Previous studies add atmospheric corrections for long baseline RTK positioning. In this section, the initial ambiguity resolution process obtains the VFS without any corrections. In this case, the equation residual will have an impact on the integer ambiguity resolution, and then Equations (7) and (8) would not be applicable.

https://doi.org/10.1017/S037346332100059X Published online by Cambridge University Press

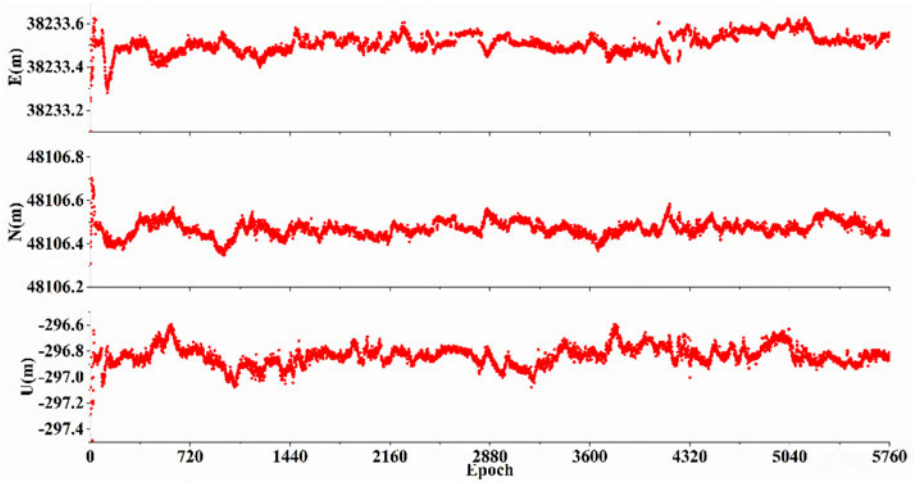


Figure 8. *Time-series scatter of Baseline 1-bjfs experiment.*

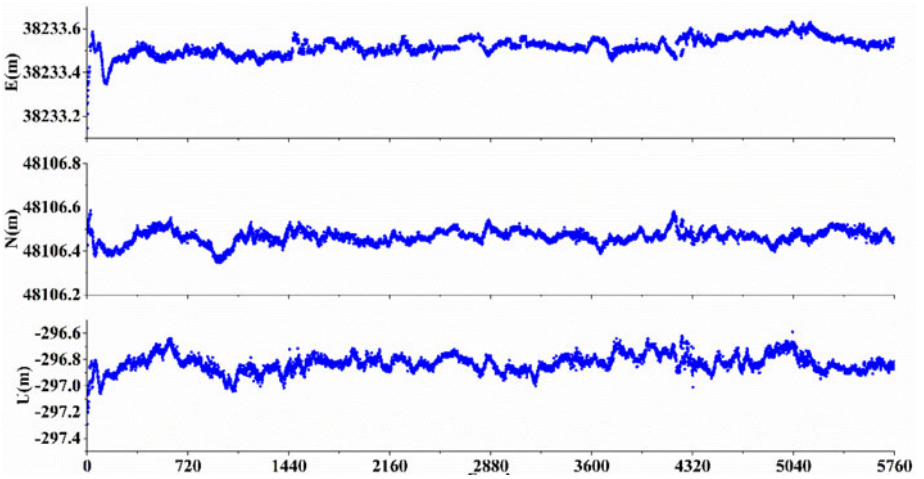


Figure 9. *VFS time series scatter of Baseline 1-bjfs experiment.*

4. Conclusions

This study attempted to apply a new strategy for the partial ambiguity resolution – the IIAR method, containing the initial ambiguity resolution and IIAR processes. The initial ambiguity resolution process is used to obtain an approximate solution, but the pseudo-range SPP float solution cannot meet the requirements. To resolve this problem, the initial ambiguity resolution process applies an iterative partial ambiguity resolution to obtain an approximate solution, which is set as the VFS. And this VFS is set as the solution of the virtual station. Previous studies applied the partial ambiguity resolution method for poorly-observed data, but its solution is unreliable when the selected satellites have poor geometry. To solve this problem, the IIAR process resolves all the adjustment equations. It is hypothesised that the virtual station and the estimated rover station have the same double-difference ambiguities in RTK positioning. With the VFS, the adjustment equations are transformed into a new form. The proposed IIAR method omits the integer ambiguity resolution for poorly-observed satellites and improves the situation in which the selected satellites have poor geometry. Three experiments were conducted to verify the proposed IIAR method. The ultra-short baseline experiment shows that the VFS is unreliable when the selected satellites have small redundancy. The short baseline experiment shows that the IIAR

https://doi.org/10.1017/S037346332100059X Published online by Cambridge University Press

method can obtain better results in some cases. And the medium baseline experiment shows that the IIAR method is not applicable for long baseline positioning.

In conclusion, it is confirmed that the proposed IIAR method is an effective tool for partial ambiguity resolution. Benefiting from the initial ambiguity resolution process, a better initial solution will be obtained under a situation of poorly-observed satellites. The IIAR process omits the ambiguity resolution for the poorly-observed satellites. The solution of the partial ambiguity resolution is unreliable when the selected satellites have poor geometry and IIAR process is then essential. Furthermore, more studies will be focused on applying the IIAR method to long baseline positioning.

Acknowledgements. This work is sponsored partially by the National Key Research and Development Project (2018YFE020091). The authors are grateful for the constructive suggestions by the anonymous reviewers.

References

Dai, L., Eslinger, D. and Sharpe, T. (2007). Innovative Algorithms to Improve Long-Range RTK Reliability and Availability. *Proceedings of the 2007 National Technical Meeting of the Institute of Navigation*, pp. 860–872.

Deng, C., Tang, W., Liu, J. and Shi, C. (2014). Reliable single-epoch ambiguity resolution for short baselines using combined GPS/BeiDou system. *GPS Solutions*, **18**(3), 375–386.

Edwards, S. J., Cross, P. A., Barnes, J. B. and Bataille, D. (1999). A methodology for benchmarking real-time kinematic GPS. *Survey Review*, **35**(273), 163–174.

Feng, Y. (2008). GNSS three carrier ambiguity resolution using ionosphere-reduced virtual signals. *Journal of Geodesy*, **82**(12), 847–862.

Ge, M., Gendt, G., Dick, G. and Zhang, F. (2005). Improving carrier-phase ambiguity resolution in global GPS network solutions. *Journal of Geodesy*, **79**(1), 103–110.

He, H., Li, J., Yang, Y., Xu, J., Guo, H. and Wang, A. (2014). Performance assessment of single- and dual-frequency BeiDou/GPS single-epoch kinematic positioning. *GPS Solutions*, **18**(3), 393–403.

Jonge, D. and Tiberius, C. (1998). The LAMBDA method for integer ambiguity estimation: Implementation aspects LGR-Series. No. 12. Technical report, Delft University of Technology, The Netherlands.

Li, J., Yang, Y., Xu, J., He, H. and Guo, H. (2015). GNSS multi-carrier fast partial ambiguity resolution strategy tested with real BDS/GPS dual- and triple-frequency observations. *GPS Solutions*, **19**(1), 5–13.

Liu, Z. (2014). *GNSS Slope Monitoring and Deformation Analysis*. Surveying and Mapping Press.

Odolinski, R., Teunissen, P. J. G. and Odijk, D. (2015). Combined BDS, Galileo, QZSS and GPS single-frequency RTK. *GPS Solutions*, **19**(1), 151–163.

Parkins, A. (2011). Increasing GNSS RTK availability with a new single-epoch batch partial ambiguity resolution algorithm. *GPS Solutions*, **15**(4), 391–402.

Paziewski, J. and Wielgosz, P. (2015). Accounting for Galileo-GPS inter-system biases in precise satellite positioning. *Journal of Geodesy*, **89**, 81–93.

Position Location and NaTeunissen, P. J. G. (1994). A New Method for Fast Carrier Phase Ambiguity Estimation. *Position Location and Navigation Symposium,* 562-573, IEEE.

Takasu, T. and Yasuda, A. (2010). Kalman-Filter-Based Integer Ambiguity Resolution Strategy for Long-Baseline RTK with Ionospheric and Troposphere Estimation. *Proceedings of the* ION GNSS *2010*, Portland, OR, USA, pp. 161–171.

Teunissen, P. J. G. (1995). The least-square ambiguity decorrelation adjustment: A method for fast GPS ambiguity estimation. *Journal of Geodesy*, **70**(1), 65–82.

Teunissen, P. J. G. (1998). Success probability of integer GPS ambiguity rounding and bootstrapping. *Journal of Geodesy*, **72**(10), 606–612.

Teunissen, P. J. G. (1999). An optimality property of the integer least-squares estimator. *Journal of Geodesy*, **73**(11), 587–593.

Teunissen, P. J. G. (2001). GNSS Ambiguity Bootstrapping: Theory and Applications. In *Proc.* KIS*2001, International Symposium on Kinematic Systems in Geodesy, Geomatics and Navigation*, Banff, Canada, Vol. 2, pp. 246–254.

Teunissen, P. J. G., Joosten, P. and Tiberius, C. (1999). Geometry-free Ambiguity Success Rates in Case of Partial Fixing. *Proceedings of the National Technical Meeting of the Institute of Navigation*. San Diego, CA. pp. 201–207.

Torre, A. D. and Caporali, A. (2015). An analysis of intersystem biases for multi-GNSS positioning. *GPS Solutions*, **19**(2), 297–307.

Wang, J. and Feng, Y. (2013). Reliability of partial ambiguity fixing with multiple GNSS constellations. *Journal of Geodesy*, **87**(1), 1–14.

Xu, P., Shi, C. and Liu, J. (2012). Integer estimation methods for GPS ambiguity resolution: An applications-oriented review and improvement. *Survey Review*, **44**(324), 59–71.

Zhang, Y., Xu, S., Wang, Z. and Zhang, X. (2001). Processing of ambiguity in GPS / GLONASS integrated positioning. *Journal of Wuhan University (Information Science Edition*, **26** (001), 58–63.

https://doi.org/10.1017/S037346332100059X Published online by Cambridge University Press

Zhang, X., Liu, J. and Li, Z. (2003). An Ambiguity Free Model for Deformation Detection with GPS. *Proceedings of the 16th International Technical Meeting of the Satellite Division of The Institute of Navigation (*ION GPS/GNSS *2003)*, Portland, pp. 2617–2621.

Zhodzishsky, M., Vorobiev, M., Khvalkov, A. and Ashjaee, J. (1998). Real-Time Kinematic (RTK) Processing for Dual-Frequency GPS/GLONASS. *Proceedings of the 11th International Technical Meeting of the Satellite Division of The Institute of Navigation (*ION GPS *1998)*, Nashville, TN, September, pp. 1325–1331.

Cite this article: Li H, Nie G, Jing W, Wu S, He Y (2022). A novel partial ambiguity method for multi-GNSS real-time kinematic positioning. *The Journal of Navigation* **75**: 3, 540–553. https://doi.org/10.1017/S037346332100059X

https://doi.org/10.1017/S037346332100059X Published online by Cambridge University Press